

Full Length Research Paper

Nanocrystalline tungsten oxide thick film sensor for the detection of H₂S gas

Nisha R^{1*}, K N Madhusoodanan¹ and V S Prasad².

¹ Dept. of Instrumentation, Cochin University of Science and Technology, Cochin 682022, India.

² Functional Materials, Material Science and Technology Division, National Institute for Interdisciplinary Science and Technology, Thiruvananthapuram 695019, India.

Abstract

Porous tungsten oxide nanocrystalline thick film sensors are prepared for the sensitive detection of H₂S gas. The sensor characteristics are investigated with respect to H₂S sensing over a temperature range 100-225^oC in air. Optimum operating temperature for H₂S sensing is found to be 200^oC. Sensor response is investigated for various concentrations and the lowest measurable concentration is found to be 7ppm. It is found that tungsten oxide based thick film sensor is a good candidate for H₂S sensors with satisfactory response and recovery times. The sensing mechanism associated with H₂S gas detection is also discussed. The prepared sensor is characterized by XRD, SEM, TEM, Raman spectroscopy and XPS.

Keywords: H₂S sensor, gas sensing, tungsten oxide, thick film sensor, metal oxide gas sensing, nanocrystalline.

INTRODUCTION

The recent concern over environmental pollution and increased awareness of the need to monitor hazardous gases has stimulated substantial interest in sensors for the gases CO, CO₂, NO_x, H₂S, etc. H₂S monitoring is particularly important in industrial environment where H₂S is usually present as an air pollutant. The presence of H₂S is not desirable because of its smell and hazards associated with it when present in high concentrations. H₂S is also liberated in nature due to biological processes and also from mines and petroleum fields. The requirement to detect and monitor these gases has led to the development of a wide variety of devices for solid-state gas sensors.

Semiconducting metal oxide gas sensors has proved to be very promising for monitoring the emission of gas species, and they represent a low-cost option to the common methods for ambient air classification, which require expensive and bulky equipment. Their sensing principle is based on the change in the resistance of a semiconductor oxide film when specific gases interact with its surface. The surface of the

semiconductor provides different surface states and when gas molecules are adsorbed and react at the semiconductor surface a change in the intergrain barrier height occurs. So, the basic principle of operation of a semiconductor gas sensor is the control of surface potential barrier by adsorbed radicals.

Metal oxide semiconductors (MOS) have been utilized as gas sensing active materials for half a century (Barsan and Weimar, 2001; Shimizu and Egashira, 1999). One of the most promising solid-state MOS chemo sensors is n-type semiconducting tungsten oxide-based gas sensor. They have demonstrated novel sensing properties such as high sensitivity, fast response time and low operation temperature. In particular, pure or doped tungsten oxide is a promising material for the detection of various substances, e.g., H₂ (Shimizu and Egashira, 1999), H₂S (Shaver, 1967; Lin et al., 1994; Solis et al., 2001), NO_x (Akiyama et al., 1991; Tamaki et al., 1994), NH₃ (Huyberechts et al., 1994; Llobet et al., 2000) and ethanol (Ionescu et al., 2005).

Furthermore, nanocrystalline materials present new opportunities for enhancing the properties and performance of gas sensors and are recognized as essential for achieving high gas sensitivity. Their surface-to-bulk ratio is much larger than that of coarse micro-grained materials, which yields a large interface

*Corresponding Author Email: rnisha.r3@gmail.com

between the oxide and the gaseous medium. Accordingly, the sensitivity of semiconductor oxide materials has been improved by reducing the particle size, and superior properties have been reported for sizes in 5–50 nm range.

In this context we have investigated the sensing characteristics of WO_3 nanoparticles to H_2S in the 7 to 200 ppm range at working temperatures of the range of 100–225°C. Semiconductor gas sensors based on nanocrystalline WO_3 powders were prepared by acid precipitation method. The thick films of the powder were coated on to glass substrate, annealed at 600°C and its response to different concentration of H_2S gas was studied. Sensor behavior is presented in detail for representative concentration of 18ppm. Our study shows that WO_3 nanoparticles are good candidates for sensing H_2S at a temperature of 200°C.

METHOD

Sensor Fabrication

The WO_3 nanoparticles were synthesized by precipitation technique from aqueous solutions of ammonium tungstate para pentahydrate (Supothina et al., 2007) $(\text{NH}_4)_{10}\text{W}_{12}\text{O}_{41}\cdot 5\text{H}_2\text{O}$, Wako) and nitric acid (HNO_3 , Merck). A predetermined amount of tungstate salt was dissolved in de-ionized water and resulting solution was brought to 80°C. With vigorous stirring, a warm, concentrated nitric acid was added drop wise. With continuous stirring the mixed solution was kept at 80°C for 30minutes. The precipitates were allowed to settle for 1 day at room temperature. Precipitate was washed by addition of a large amount of de-ionized water into precipitate followed by stirring for about 10 minutes and allowing precipitates to settle down before decanting the liquid. This washing procedure was carried out six to seven times. The precipitates were dried at 100°C overnight and then calcined in air at a temperature of 400°C for 6hrs. The calcined precipitate was finely powdered in a mortar. For sensor preparation the powder were dispersed in methanol and painted on to a glass substrate. Thus a thick film of the sensor material was obtained. The sensor was then annealed at a temperature of 600°C overnight prior to the temperature dependent measurements.

Gas sensing set up

The gas sensing measurements of the thick film sensor were tested on indigenously developed static gas characterization system. The test system consisted of a stainless steel chamber of diameter 7.5cm and 6.35cm height. Effective volume of the chamber was 280ml. An inlet was provided for inserting desired concentration of gas to the chamber. An outlet is also provided to remove

the gas. The pre-calibrated gas cylinders were obtained from laboratories. The gas was injected into test chamber with a syringe through an inlet provided with septum. Electrical connections from the sensor were made using two thin copper wires, bonded to the sensor with silver paint. The sensing capability of the sensor was characterized at different operating temperatures to find out optimum working temperature. A heater is incorporated in the chamber in order to heat sample to desired temperature. A resistance temperature detector (RTD) is used to sense temperature. Feedthroughs are provided on the top of the chamber for electrical connections to the heater as well as for the temperature sensor (RTD). A microcontroller based PID temperature controller was used to control the operating temperature of the sensor to an accuracy of 0.5°C. Electrical characterization of the WO_3 thick films in presence of the gas were obtained by measuring the change in resistance of films. A Keithley 195A digital multimeter is used to measure the resistance of the sensor which is interfaced to the system by a GPIB interface. The programming for the interface is done using BASIC language.

Characterization

The crystalline structure and particle size of the as prepared powder sample and 600°C annealed thick film sensor were examined by X-ray diffraction measurement (XRD, Bruker AXS D8 Advance). The crystallite size (D) was calculated from peak broadening using the Scherrer approximation, which is defined as

$$D = \frac{0.9\lambda}{B \cos \theta} \quad (1)$$

Where λ is the wavelength of the X-ray (1.5418 Å), B is the full width at half maximum (FWHM, radian) and θ is the Bragg angle (degree). Raman spectra of 600°C annealed WO_3 thick film sensor was obtained using Horiba Jobin Yvon LabRam HR system at a spatial resolution of 2 mm in a backscattering configuration. The 514.5 nm line of Argon ion laser was used for excitation. Surface morphology and compositional analysis of thick films were examined using scanning electron microscopy (SEM, JEOL Model JSM - 6390LV). TEM (FEI, TECNAI 30G2 S-TWIN microscope) image of 600°C overnight annealed sensor powder was also obtained. The electronic structure of the surface of WO_3 was performed by X-ray photoelectron spectroscopy (XPS) with a SPECS GmbH spectrometer (Phoibos 100 MCD Energy Analyzer) using MgK α radiation (1253.6eV).

RESULTS AND DISCUSSION

Structural characterization

Figure 1 shows the XRD spectra of as prepared precipi-

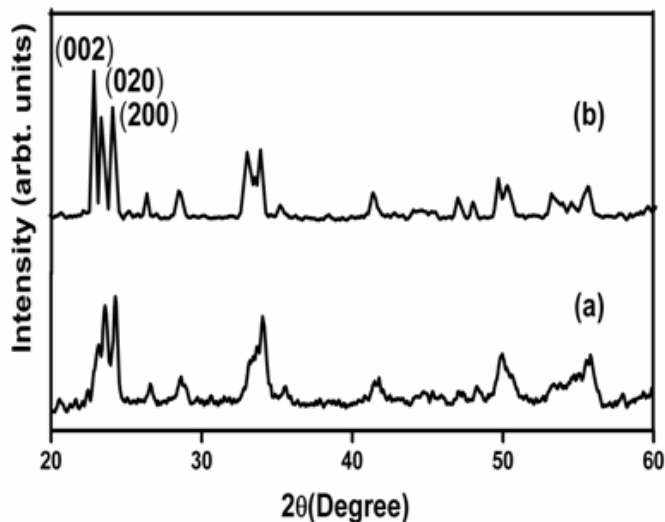


Figure 1. XRD patterns (a) WO_3 precipitate calcined at 400°C for 6 hr (b) thick film sensor annealed at 600°C overnight

tate calcined in air at a temperature of 400°C for 6hr and thick film sensor of WO_3 annealed at 600°C overnight. Main peaks were found at $2\theta = 23.0^\circ$, 23.6° and 24.3° , which were identified as corresponding to Miller index (002), (020), and (200), respectively, in triclinic WO_3 (JCPDS# 20-1323). Hence the 600°C overnight annealed powder was identified by XRD as nanocrystalline WO_3 . Using Scherrer equation average crystallite size of the WO_3 thick film sensor were found to be 30nm.

Raman spectrum of 600°C annealed tungsten oxide thick film sensor is shown in figure 2. The spectrum can be divided into three main regions at $900\text{--}600$, $400\text{--}200$ and below 200cm^{-1} . Peaks below 200cm^{-1} are associated with lattice modes, the intermediate frequencies ($200\text{--}400\text{cm}^{-1}$) showing O–W–O bending mode features, and the last at higher frequencies ($600\text{--}900\text{cm}^{-1}$) with the peaks related to W–O stretching modes (Baserga et al., 2007).

Typical surface morphology of thick film sensor annealed at 600°C overnight is shown in figure 3. It is evident that the material consists primarily of crystalline aggregates and is highly porous in nature. The most important factors that influence the sensor characteristics are probably microstructure and surface area. The films exhibiting a porous structure have a large fraction of atoms residing at surfaces and interfaces between the pores, which suggests that the microstructure of the films is suitable for gas-sensing purposes. The energy dispersive X-ray analysis, which is shown in the inset, reveals that only oxygen and tungsten elements are present.

Figure 4 show TEM image of the 600°C annealed thick film sensor WO_3 powder. TEM image also confirms that sensor consists of crystalline aggregates and nanoparticle prepared is spherical in nature. TEM results support particle size obtained by XRD characterization.

In order to understand the chemical composition of tungsten oxide film, we carried out XPS measurement. XPS spectrum of the 600°C annealed sample is illustrated in figure 5. The W 4f core level spectrum recorded on 600°C annealed samples shows the two components associated with W 4f_{5/2} and W 4f_{7/2} spin orbit doublet at 36.8 and 34.9eV. Binding energy values obtained for the spin orbits shows a small shift towards the lower binding energy. This shift may be caused by the contribution from W⁵⁺ or W⁴⁺ states, resulting in oxygen vacancies in thick film sensor (Moulzolf et al., 2001). The O1s peak is located at 529.7eV, which is ascribed to the W–O peak.

H₂S gas response studies

Gas sensing capability of thick film sensors were measured to reducing gas H₂S in air at a temperature range 100 to 250°C . Sensors were not sensitive to test gas at room temperature. In general, it is known that the metal oxide sensor is affected by the working temperature. The higher temperature enhances surface reaction of the sensor and gives higher sensitivity in a temperature range. Amount of chemisorbed oxygen on surface and the surface species available for adsorption highly influences the change in conductivity (Mizsei, 1995). At lower temperature, oxygen species on film surface are not active; hence a low interaction happens between adsorbed oxygen species and detected H₂S gas. Thus the response of the WO_3 thick film sensor is low at lower temperature. At higher temperature some of adsorbed oxygen species may be desorbed from the film which contributes to low response value. As a result, there should be an optimal operating temperature to balance the above two effects in order to achieve maximum gas response.

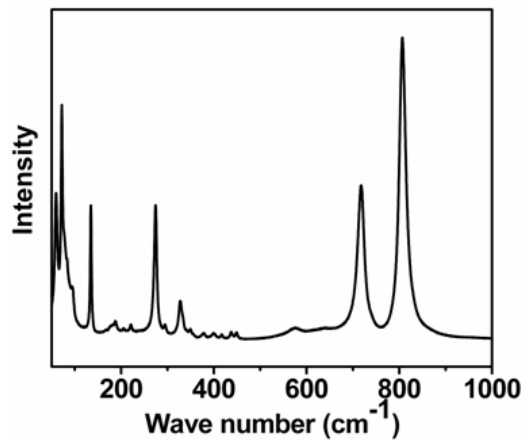


Figure 2. Raman spectra of 600°C annealed tungsten oxide thick film sensor.

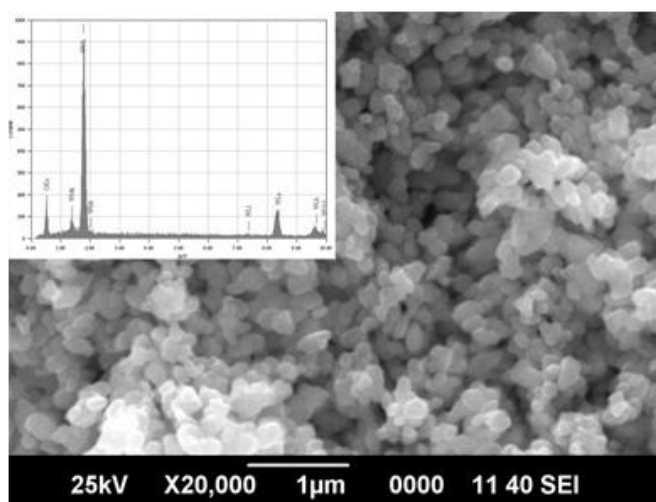


Figure 3. SEM image of the WO₃ thick film sensor annealed at 600°C with inset showing EDS spectrum.

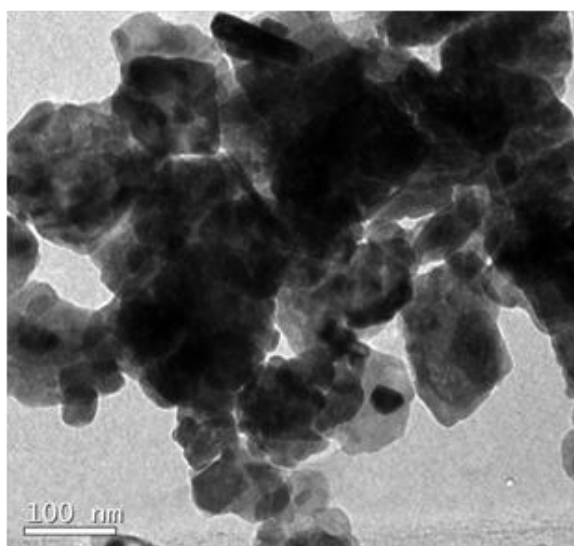


Figure 4. TEM image of the WO₃ thick film sensor annealed at 600°C.

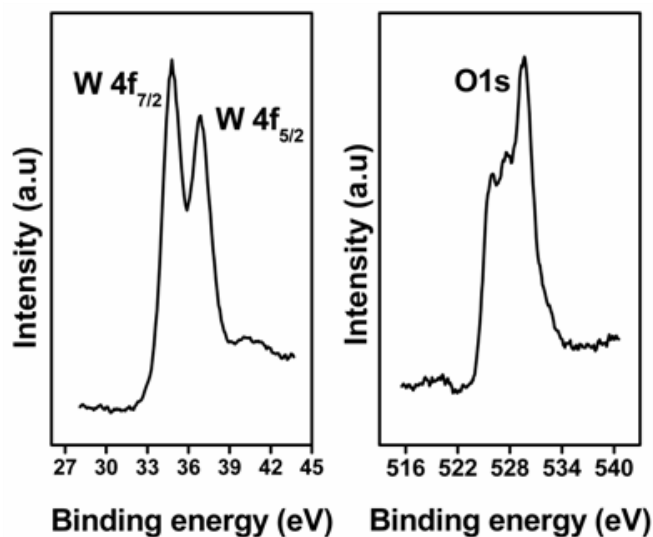


Figure 5. XPS spectrum of the 600°C annealed sensor

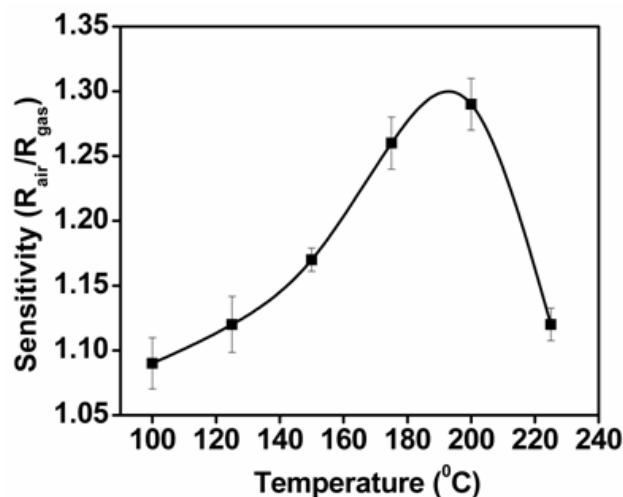


Figure 6. Temperature dependent sensitivity to a concentration of 18ppm

Samples were exposed to variable concentrations in the range 7 to 200ppm. Since WO_3 is an n type semiconductor resistance decrease on exposure to reducing gas like H_2S . Sensor sensitivity is defined as $S=R_{air}/R_{gas}$, where R_{gas} is resistance of sensor in presence of gas and R_{air} is resistance of sensor before introduction of gas. Response time is defined as time required for resistance to reach 90% of equilibrium value after test gas is injected. Recovery time is time necessary for sensor to attain a resistance of 10% of original value in air. Gas sensing characteristics of thick film sensor to a concentration of 18ppm studied is discussed in detail. Similar results were obtained for higher concentrations studied. Response of sensor at different operating temperature to a concentration of 18ppm is shown in figure 6.

Response and recovery time sensor characteristics to 18ppm concentration studied is illustrated in figure 7.

Temperature dependent sensitivity shown in figure 6 indicates that as temperature increases response of sensor increases reaching a maximum value and then decreases. At lower temperatures recovery time mounted to several minutes and sensitivity was also very low. These sensor characteristics could be significantly enhanced by having the sensor operate at higher temperature. An operating temperature of 200°C was considered as optimum operating temperature since best compromise between sensor sensitivity and sensor dynamics is obtained at this temperature. A further increase of working temperature reduces sensitivity of sensor. At this operating temperature sensor is found to have a maximum sensitivity of 1.3 with a response time of 22 seconds and recovery period of about 4.1 minutes.

Figure 8 illustrates reduction in resistance on introduction of 18 ppm concentration of gas at 100°C, 150°C, 200°C and 225°C. It is evident that injection of

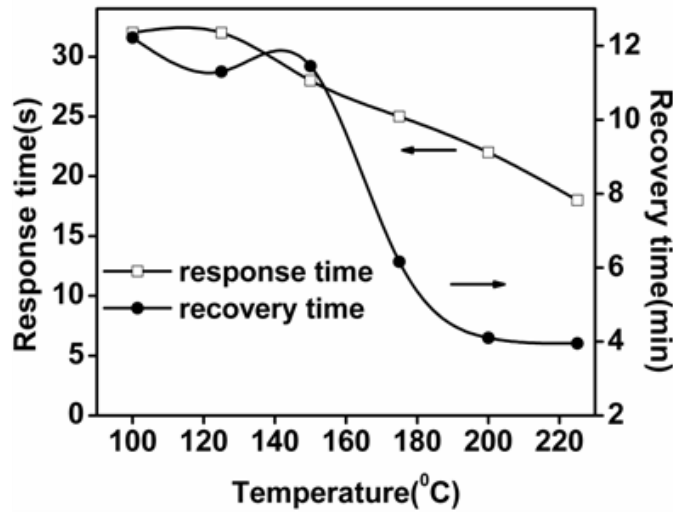


Figure 7. Response and recovery characteristics of WO₃ thick film sensor at different operating temperature to 18ppm of H₂S gas

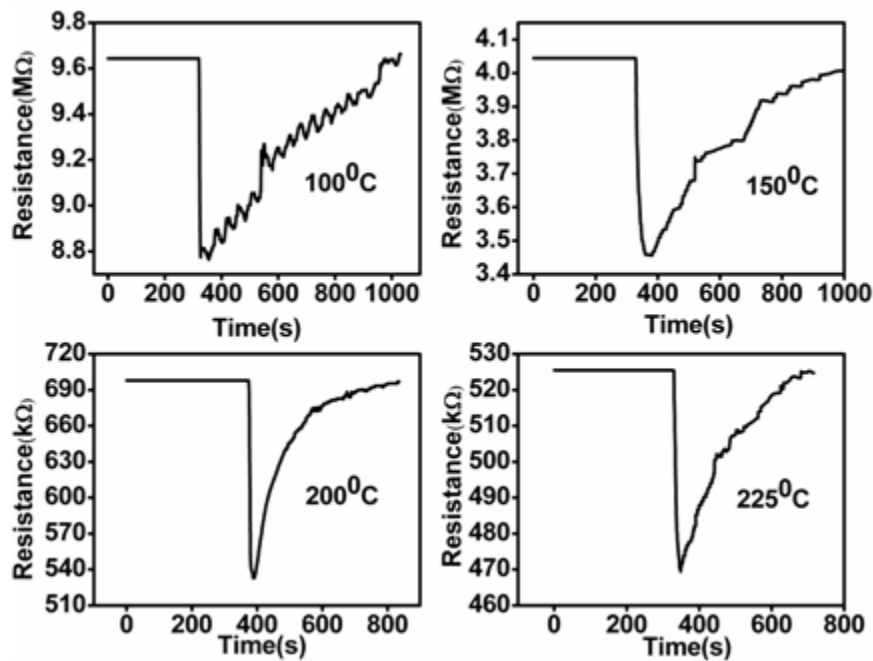


Figure 8. Resistance variation of thick film WO₃ sensor to 18 ppm H₂S gas concentration at different operating temperatures

gases in the test chamber induces a measurable change in electrical resistance, which returns to its initial value when sample is exposed to pure dry air. This proves that adsorption process is reversible. It is known that interaction between metal oxide and adsorbed gas is a dynamic process. When film is exposed to a test gas in air, adsorption and desorption processes occur simultaneously. In response process adsorption dominates on desorption process until stationary conditions are attained. In this situation number of adsorbed gas molecules will be equal to number of

desorbed ones, and electrical conductivity attains a constant value. After test gas is cut off, desorption prevails on re-adsorption process and conductivity will return to its original value. Sensitivity of sensor to different concentration studied at optimum temperature of 200°C is illustrated in figure 9. Resistance variation on introduction to different concentration of test gas is shown in figure 10.

It is known that sensing mechanism of oxide materials is surface controlled in which grain size, surface states and oxygen adsorption play an important

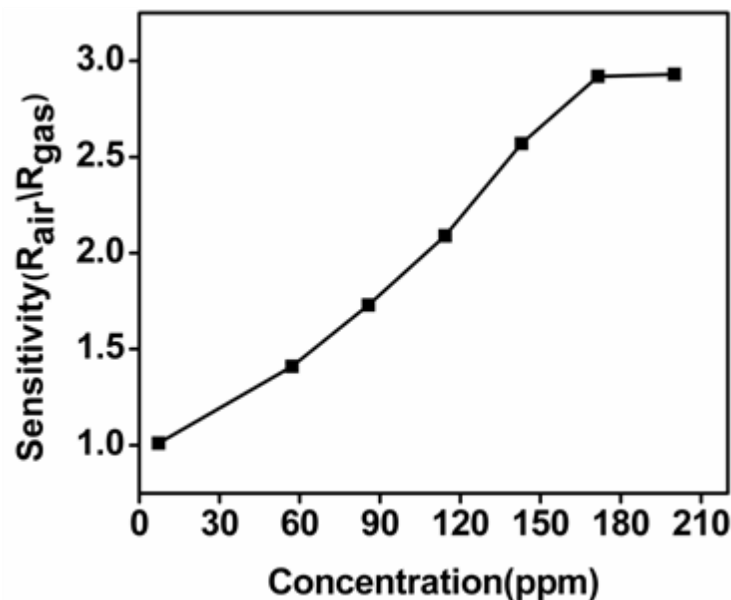


Figure 9. Sensitivity of sensor to different concentration at optimum temperature of 200°C

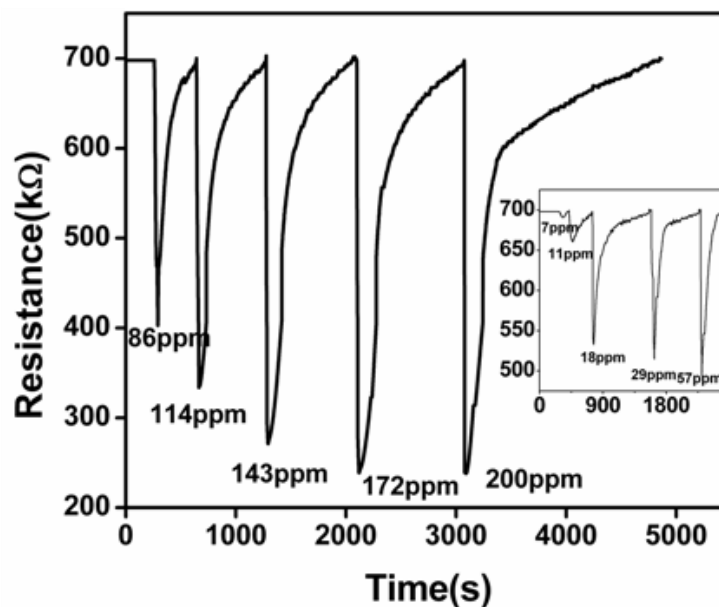


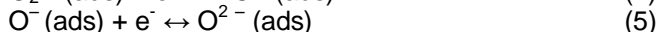
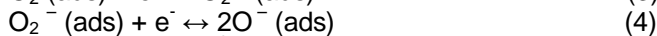
Figure 10. Resistance variation on introduction of different concentration of test gas

role (Rothschild and Komem, 2004). The larger surface area generally provides more adsorption-desorption sites and thus higher sensitivity. The sensor element consists of semiconductor nanoparticle. The microstructure and morphology of these aggregates are considered to be very important for the transducer function. Each particle is connected with its neighbors either by grain-boundary contacts or by necks. In the case of grain-boundary contacts, electrons should move across the surface potential barrier at each boundary. The change of the barrier height makes the electric

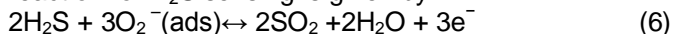
resistance of the element dependent on the gaseous atmosphere, as first pointed out by Ihokura 1983. The resistance, and hence the gas sensitivity, in this case are not basically dependent on the particle size. In the case of necks, electron transfer between particles takes place through a channel which is formed inside the space-charge layer at each neck. The width of the channel is determined by the neck size and thickness of the surface charge layer (L) and its change with gases gives rise to the gas-dependent resistance of the element, as first pointed out by Mitsudo, 1980. Obviously

the gas sensitivity in this case is dependent on the particle size. These two models, although rather conceptual, indicate the importance of the microstructure for the transducer function of the element. Tamaki et al. 1994 studied the grain size effects in WO_3 for nitrogen oxide detection. The results indicate that for a crystallite size greater than 30nm the conduction is under grain boundary control. The average crystallite size of pure and copper doped WO_3 is in the range of 30-33nm. Hence we deduce that in our sensors the conduction is through grain boundary contacts.

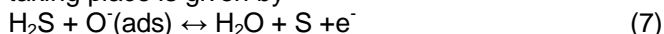
Annealing temperature of the sensor is another contributing factor to the sensitivity of sensor. Higher temperature annealing can create oxygen deficiency on the surface of films thereby creating more adsorption sites for target gas as well as adsorbed oxygen. Studies on operation mechanism of semiconductor gas sensors indicate that most target gases are detected due to influence of adsorbed oxygen. Atmospheric oxygen gets adsorbed on surface of metal oxide removing electrons from conduction band of sensing metal oxide and occurs on surface in form of O^- , O_2^- and O_2^- creating a thin layer of depletion region at the surfaces of WO_3 grains (Schierbaum et al., 1991). The reaction is as follows where (gas) denotes gaseous phase and (ads) denote adsorbed species respectively.



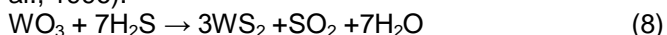
Reaction (3) usually occurs at temperature below 175°C and reactions (4) and (5) occur at temperature above 175°C . The adsorbed oxygen species play a crucial role in H_2S sensing. At lower temperature reaction for H_2S sensing is given by



For higher temperature operation, the reaction taking place is given by



According to Equation (3), (4) and (5), oxygen adsorption reaction occurs prior to H_2S sensing, creating a thin electron-depleted layer at the surface of WO_3 . As H_2S is adsorbed, electrons are released into conduction band according to Equation (6) and (7). Hence resistance of WO_3 sensor decreases and hence conductivity increases on interaction with H_2S gas. Another reaction that can play a role in gas sensing is formation of additional surface oxygen vacancies, created due to interaction with test gas (Fruhberger et al., 1996).



The above reaction takes place on surface and involves a reduction of W^{6+} to W^{4+} . Oxygen leaves surface thereby releasing electrons into the grains so that conductivity of film is increased. Further, reoxidation of vacancies by O_2 results in a competition with formation of oxygen vacancies by H_2S .

At lower temperature sensitivity as well as recovery characteristics is very poor. Low sensitivity of sensor at lower operating temperature is due to slow reaction kinetics between H_2S and adsorbed oxygen ions. Long recovery time is due to incomplete desorption of adsorbed reaction products and H_2S after exposure to test gas. As the temperature is increased reactions described by equation (3), (4), (6) and (7) as well as desorption of products are faster, which explains the increase of sensitivity and decrease in recovery time. At temperatures above 200°C sensor exhibits reduced sensitivity. This is due to higher desorption rate than adsorption process that occur on surface of thick film sensor.

CONCLUSION

Sensitive layers of tungsten oxide were prepared by dispersing the prepared tungsten oxide powder in methanol and drop casting on glass substrates followed by overnight annealing at 600°C . The obtained crystalline phase of WO_3 nanoparticles was triclinic in nature. The structure of sensor was characterized using XRD. The surface morphology and elemental composition were characterized by scanning electron microscopy and energy dispersive X-ray analysis. It was found that the WO_3 samples consisted of crystalline aggregates. This was confirmed in TEM results. The particles were spherical in nature. Gas sensing properties of samples were studied for the detection of H_2S gas. Resistance of the films decrease upon exposure to gases and attained a saturation value. Sensor regains its original value after test gas is removed. Sensor exhibit good sensing characteristics to H_2S in the concentration range studied, 7 to 200 ppm over the temperature range $100-125^\circ\text{C}$. The best results were obtained at operating temperature of 200°C with a sensitivity of 1.3. Response and recovery time of sensor at this optimum temperature was 22 seconds and 4.1 minutes respectively. Lowest measurable concentration is found to be 7ppm. Resistance always returned to its initial value after the test gas is shut off for all concentration studied. Results indicate that response of sensor is reproducible during this test. The different sensing mechanisms associated with H_2S sensing is also discussed

ACKNOWLEDGEMENTS

The authors wish to acknowledge Dr. M.K. Jayaraj, Nanophotonic and Optoelectronic Devices laboratory, Dept. of physics for Raman measurements under DST nano mission initiative programme and Dr. Prof. G. Mohan Rao, Department of Instrumentation and Applied Physics, Indian Institute of Science, Bangalore for XPS

measurement. We are thankful to SAIF, Cochin University of Science and Technology, Kochi, Kerala, India for the XRD and SEM measurements.

REFERENCE

- Akiyama M, Tamaki J, Miura M, Yamazoe N (1991). Tungsten oxide-based semiconductor sensor highly selective to NO and NO₂ Chem. Lett. 1, 1611-1614.
- Barsan N, Weimar U (2001). Conduction model of metal oxide gas sensors, J. Electroceram. 7143-167.
- Baserga A, Russo V, Fonzo FD, Bailini A, Cattaneo D, Casari CS, Bassi AL, Bottani CE (2007). Nanostructured tungsten oxide with controlled properties: Synthesis and Raman characterization, Thin Solid Films 515, 6465 -6469.
- Fruhberger B, Grunze M, Dwyer DJ (1996). Surface chemistry of H₂S-sensitive tungsten oxide films Sensors and Actuators B 31, (1996). 167-174.
- Huyberegts G, Muylder MV, Honore M, Desmet J, Roggen J (1994). Development of a thick film ammonia sensor for livestock buildings, Sensors and Actuators B 18, 296-299.
- Ihokura H (1983). SnO based inflammable gas sensors Doctoral Thesis Kyushu University Japan.
- Ionescu R, Hoel A, Granqvist CG, Llobet E, Heszler P (2005). Low level detection of ethanol and H₂S with temperature-modulated WO₃ nanoparticle gas sensors Sensors and Actuators B 104, 132 - 139.
- Lin HM, Hsu CM, Yang NY, Lee PY, Yang CC (1994). Nanocrystalline WO₃-based H₂S sensors, Sensors and Actuators B 22, 63-68.
- Llobet E, Molas G, Molinàs P, Calderer J, Vilanova X, Brezmes J, Sueiras JE, Correig X (2000). Fabrication of highly selective tungsten oxide ammonia sensor, J. Electrochem. Soc. 147, 776-779.
- Mitsudo H (1980). Ceramics for gas and humidity sensors gas sensor, Ceramics 15, 339-345.
- Mizsei J (1995). How can sensitive and selective semiconductor gas sensors be made Sensors and Actuators B 23, 173-176.
- Moulzolf SC, Ding S, Lad RJ (2001). Stoichiometry and microstructure effects on tungsten oxide chemiresistive films Sensors and actuators B 77, 375-382.
- Rothschild A, Komem Y (2004). The effect of grain size on the sensitivity of nanocrystalline metal-oxide gas sensors, J. Appl. Phys. 95, 6374 -6380.
- Schierbaum KD, Weimar U, Göpel W, Kowalkowski R (1991). Conductance, work function and catalytic activity of SnO₂-based gas sensors Sensors and Actuators B 3, (1991) 205-2014.
- Shaver PJ (1967). Activated tungsten oxide gas detectors, Appl. Phys. Lett. 11, 255-257.
- Shimizu Y, Egashira M (1999). Basic aspects and challenges of semiconductor gas sensors, MRS Bull. 24, 18-24.
- Solis JL, Saukko S, Kish LB, Granqvist CG, Lantto V (2001). Nanocrystalline tungsten oxide thick films with high sensitivity to H₂S at room temperature, Sensors and Actuators B 77, 316 -321.
- Supothina S, Seeharaj P, Yoriya S, Sriyudthsak M (2007). Synthesis of tungsten oxide nanoparticles by acid precipitation method Ceramics International 33, 931-936.
- Tamaki J, Zhang Z, Fujimori K, Akiyama M, Harada T, Miura N, Yamazoe N (1994). Grain-size effects in tungsten oxide-based sensor for nitrogen oxides, J. Electrochem. Soc. 141, 2207-2210.

How to cite this article: Nisha R, Madhusoodanan KN, Prasad VS (2014). Nanocrystalline tungsten oxide thick film sensor for the detection of H₂S gas. Int. J. Environ. Sci. Toxic. Res. Vol. 2(3):55-63